Turk J Elec Eng & Comp Sci, Vol.19, No.3, 2011, © TÜBİTAK
doi:10.3906/elk-0912-332

Experimental analysis of an alternator excited with photovoltaic cells for small power plants

Kamil Rıfat İrfan GÜNEY[1], **Nevzat ONAT**[2,*]
[1] *Department of Electrical Engineering, Acıbadem University, Gülsuyu Mah. Fevzi Çakmak Cd. Divan Sk. No. 1, Maltepe 34742 İstanbul, TURKEY*
e-mail: irfan.guney@acibadem.edu.tr
[2] *Vocational School of Technical Studies, Electrical Program, Göztepe Campus, Marmara University, Kadıköy 34722 İstanbul, TURKEY*
e-mail: nonat@marmara.edu.tr

Received: 24.12.2009

Abstract

In this study, an automatic voltage regulator fed by photovoltaic (PV) cells was designed for use in small power alternators. The design aimed to increase the energy output of the alternator and to ensure necessary current output from the PV cells to support the synchronous generator excitation system. For energy transformation from small renewable energy sources, designers have favored the use of alternators that produce higher quality electric power, rather than asynchronous generators. We also address the designed system's suitability for real-life application, examining the steady-state performance of the photovoltaic cell excited alternator (PVCEA) with various loads and its behavior in sudden load and fault situations.

Key Words: *Photovoltaic cell, alternator, small power plants, synchronous generator, fault analysis*

1. Introduction

There is much interest at present in the hybrid operation of photovoltaic (PV) cell systems with conventional or other renewable energy systems, to increase the energy productivity of small hydroelectric or wind stations and power electrically operated motors with PV cells. Most studies have examined synchronous generators for energy transformation in energy production systems, studying the automatic voltage and speed regulators of such machines. The stability of power systems after a fault or sudden load mostly depends on the behavior of the alternators feeding the system. For this reason, it is necessary to examine the behavior of power system stabilizers during their steady-state operation as well as in response to sudden loads and faults [1-7].

Borowy used a 1.5-kW wind energy system with a synchronous generator and a 2.5-kW photovoltaic hybrid system to feed a load without a grid connection. Power obtained from both sources was stored and transmitted to the receiver through an inverter circuit. The dynamic performance of the system was analyzed,

*Corresponding author: Vocational School of Technical Studies, Göztepe Campus, Marmara University, Kadıköy, 34722, İstanbul-TURKEY

both theoretically and experimentally, during sudden wind gusts and over random cloud movements [8]. Giraud observed the operation of a hybrid wind-PV cell system in parallel to the national network on the same system. [9].

Vasinanukom performed a study that used a direct current (DC) motor-synchronous generator in a laboratory for the purpose of simulating the turbine-generator system. By assuming that a motor-generator system carries the same properties as a real power station, he was able to create LabVIEW programs to simulate turbine speed and excitation control [10]. Ehnberg and Bollen analyzed the reliability of hybrid PV cells and small hydroelectric stations. The hybrid operation of PV cells with an alternator was examined in that study and presented as an alternative to conventional diesel generators that are used to obtain energy in remote regions. Reliability in PV cell systems operating individually is very low (typically below 50%) due to cloud motion, but reliability was shown to increase considerably with the addition of a hydroelectric station containing a small loading pool. The study also examined the effects of including a battery in the system. A similar study in Indonesia monitored the performance of and operation of a system consisting of a PV cell and hydroelectric station [11, 12].

PV cells often feed a load possessing electric machine coils, especially in systems such as pumping and cooling. For this reason, it is very important to understand the performance of PV cells with such loads. In a separately excited DC motor with both coils fed by PV cells, it is possible to obtain a fixed speed by controlling both coils [13]. Vongmanee performed a study on the operation of a 3-phase asynchronous motor with PV cells, where DC from the cells was transformed to AC through a 3-phase inverter circuit. The vector control technique was used for asynchronous motor speed control and the resulting behavior of the system was examined [14].

2. System description

In this study, a synchronous generator was excited with voltage obtained from PV cells. Voltage and speed controllers were used to keep the system stable. For this purpose, the photovoltaic cell excited alternator (PVCEA) was subjected to various loads while the output voltage and frequency were kept within predetermined values.

The quality of electric power is measured by the extent to which the amplitude and frequency of voltage remain constant. For this reason, electric generators must maintain this stability within certain limits. Fluctuations in frequency negatively affect the recipients of the electricity. Modern electronic home appliances often operate with a reference frequency that they themselves establish, and thus are not greatly affected by changes in frequency. However, electric motors are negatively affected by frequency changes. Commonly used asynchronous motors and transformers will overheat easily at low frequency because they will attract high magnetizing currents. For this reason, the frequency must not fall below the lower limit of the motor's specifications. An increase in frequency does not cause a significant problem for such motors up to a certain point, usually around 10%-20% above the nominal frequency. Magnetizing current decreases, and output increases. In addition, an increase in speed improves the cooling of rotating motors [5, 15].

The specifications of the PV cells and DC motors used in our experiments are given in Table 1. The DC motor given in the table was used to simulate the turbine system.

The parameters obtained from our experiments on synchronous generators are given in Table 2. The block diagram of the experimental design is given in Figure 1. For the PV cell excitation system, we used 4 photovoltaic modules supplying 125 W each to feed an inverter with a rating of 500 W. Energy storage was

provided by 2 12-V, 100-Ah batteries connected in a series. The cable from the cells to the battery was 10 mm^2 of copper, that from the battery to the charge regulator and inverter was 6 mm^2 of copper, and 2.5 mm^2 of copper was used after the inverter outlet. In this study, the model is a stand-alone photovoltaic system. Therefore, the number of modules to be used and the battery capacity was calculated for the stand-alone system located in İstanbul. Calculation details are given in the appendix.

Table 1. Specifications of tested PV cells and DC motors.

Photovoltaic Module					
Serial Number	U_{sys}	U_{mpp}	I_{mpp}	U_{OC}	UI_{SC}
Schüco EB03070A077946	600 V	18.8–19.1 V	6.63–6.85 A	2–24.3 V	7.27–7.38 A
D. C. Motor					
Serial Number	Rated Power	Armature Voltage	Armature Current	Excitation Voltage	Excitation Current
Terco 9199	2 kW	220 V	12 A	220 V	0.8

Table 2. Parameters of synchronous generator.

Rated Power	1.2 kVA	d-axis transient reactance (X'_d)	25.562 Ω/phase
Excitation	220 V / 1.4 A	q-axis transient reactance (X'_q)	22.9871 Ω/phase
Frequency	50 Hz	d-axis subtransient reactance (X''_d)	6.881 Ω/phase
Stator resistance (R_e)	2.084 Ω/phase	q-axis subtransient reactance (X''_q)	21.442 Ω/phase
Phase voltage (V)	127 V	Outer stator radius	186 mm
Phase Current (I)	3.5 A	Outer rotor radius	106 mm
d-axis reactance (X_d) q-axis reactance (X_q)	40.455 Ω/phase 22.9871 Ω/phase	Air gap width Axial length	4 mm 130 mm

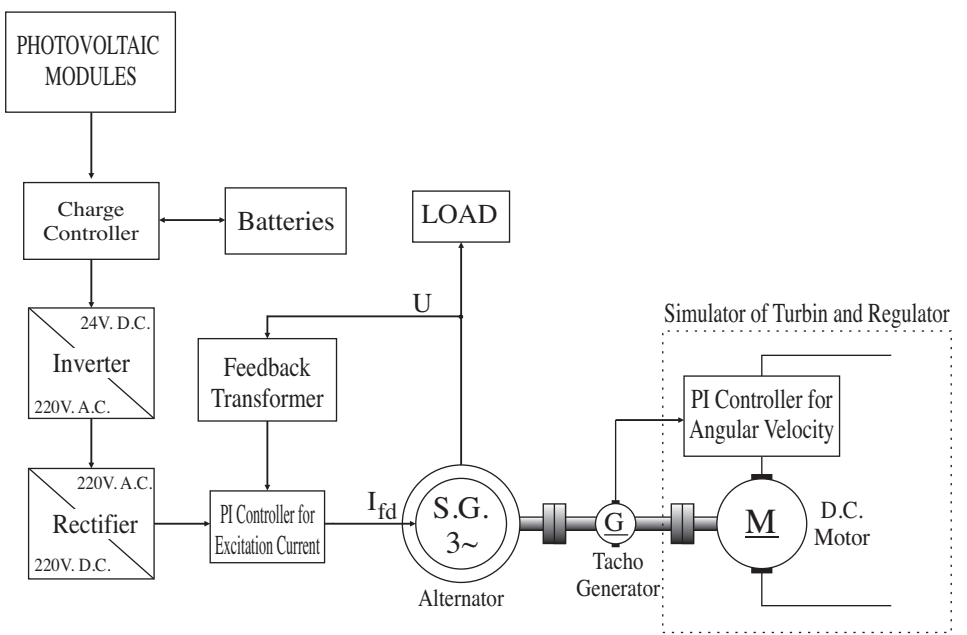

Figure 1. Block diagram of experimental setup.

3. Applications and measurements

In the first stage of the experimental applications, we examined the voltage and frequency responses of the PVCEA against resistive, inductive, and asynchronous motor loads in continuous operation. In the second stage, we observed the behavior of the system after such loads were added to and removed from the circuit. In the last stage, we plotted graphs of voltage and frequency resulting from a 3-phase symmetric short circuit and a 1-phase soil short circuit. In the sudden loading and fault experiments, voltage and frequency measurements were taken with a multiplexer device that can make measurements in intervals of 0.1 s. The multiplexer device was connected to a computer via an RS-232 serial communication system to record the data. The graphs were drawn after making the unit value conversion. All connections and values of the loads are given in the appendix.

3.1. Resistive load

Resistance loading experiments for the PVCEA were performed with 7 grade-adjusted load units with 1.2 kW of total power. In the steady-state experiment, loads were connected into the circuit one at a time, and the change in voltage and frequency with each additional load was examined. As shown in Figure 2, the controllers were held at constant voltage and frequency in response to increasing loads. Excitation current was provided by PV modules continuously increased and the power factor remained stable at a 0° angle ($\mathrm{Cos}\varphi = 1$) because of the ohmic load (Figure 3).

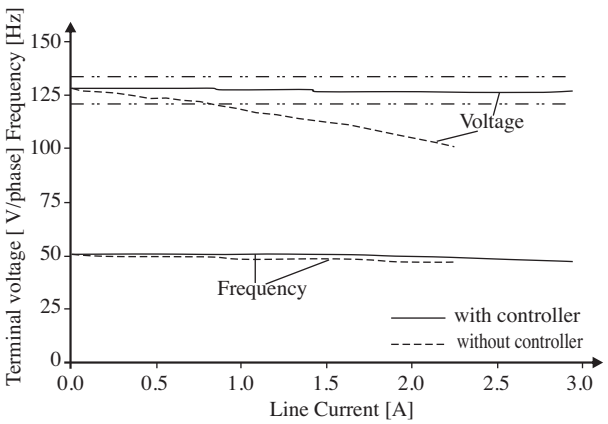

Figure 2. Steady-state performance of PVCEA under resistive load.

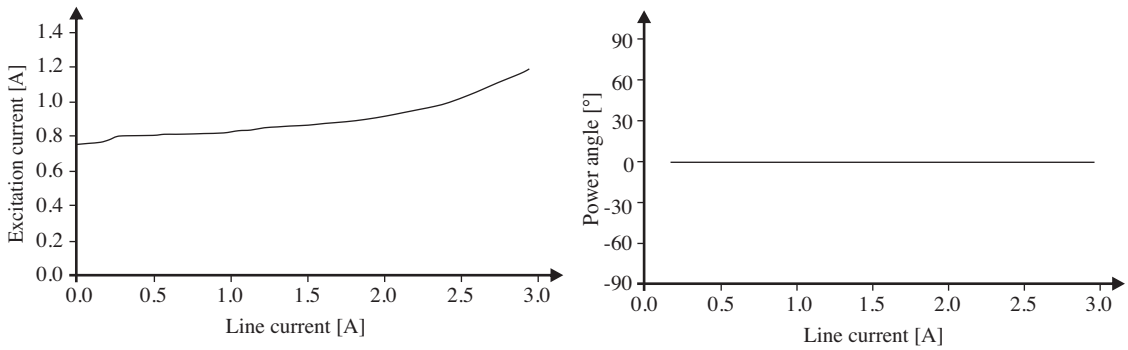

Figure 3. Excitation current and power angle characteristics of PVCEA (with controller).

In the case of the connection of a sudden nominal resistive load, the fluctuations of voltage and frequency were damping in a period of approximately 0.5 s. This process was a little longer during the disconnection of the load (approximately 0.8 s) (Figure 4).

3.2. Inductive load

For the case of an inductive load situation, we used a load model with a serial-triangle connection of 2 load units of 7 grades, with a total reactive power of 900 VAr. Pure inductive load is the worst situation in terms of voltage stability. The largest positive voltage regulation occurs in inductive loads. This effect is clearly seen in the increase in load without the controller. As shown in Figure 5, voltage regulation was found to be approximately 40% in the case of only a half-load. Designed controllers kept the system stable in a steady-state operation with nominal inductive load. Because of the load characteristics, the excitation current exceeded the nominal value and the power angle remained stable at approximately 88° (Figure 6).

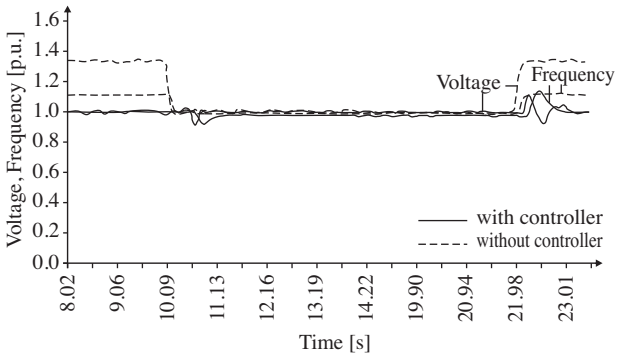

Figure 4. Transient voltage and frequency response of PVCEA under instantaneous resistive load connection and disconnection.

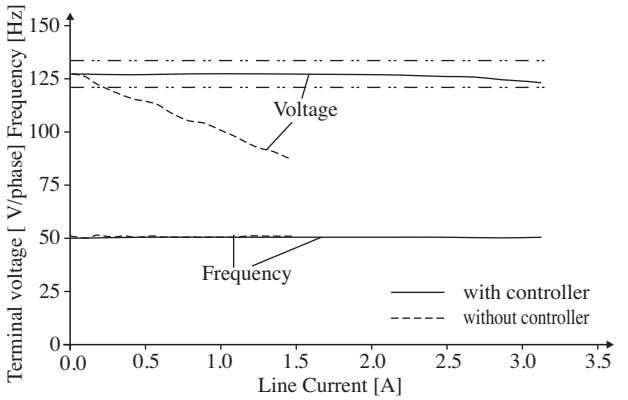

Figure 5. Steady-state performance of PVCEA under inductive load.

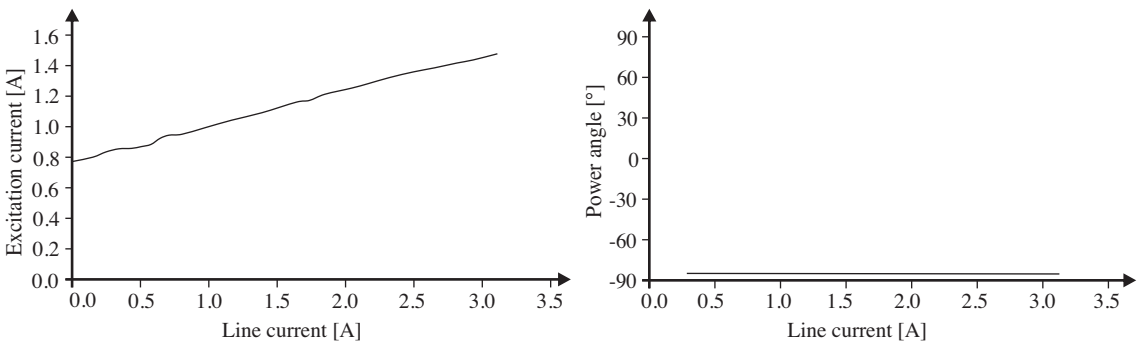

Figure 6. Excitation current and power angle characteristics of PVCEA under inductive load (with controller).

The obtained results for instantaneous connection and disconnection of the nominal inductive load can be seen in Figure 7. Exceedance and reduction of voltage that occurred during both switching process were higher in proportion than the resistive load. However, stabilization of the system time was under 1 s. Because the active power consumption of the inductive load was very small, there was virtually no change in frequency.

3.3. Induction motor load

Generators are usually subjected to a combined R-L load during operation. This load situation is established collectively by recipients through electric motors and fluorescent lamps. To examine the steady-state and transient responses of the PVCEA to an induction motor load, a 1.1-kW slip ring motor was used. As shown in Figure 8, an induction motor load has very compelling attributes for alternators. However, even under this load, controllers were held to a high quality energy that had constant voltage and frequency in steady-state operation. As a result of the increase in motor shaft load, the power angle decreased from 75° to 60°. Thus, the power factor and efficiency of the system were improved (Figure 9).

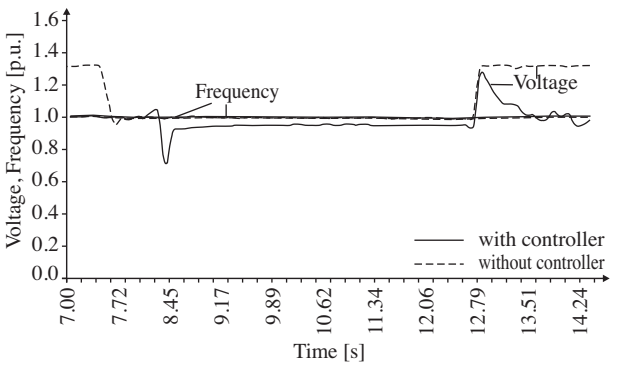

Figure 7. Transient voltage and frequency response of PVCEA under instantaneous inductive load connection and disconnection.

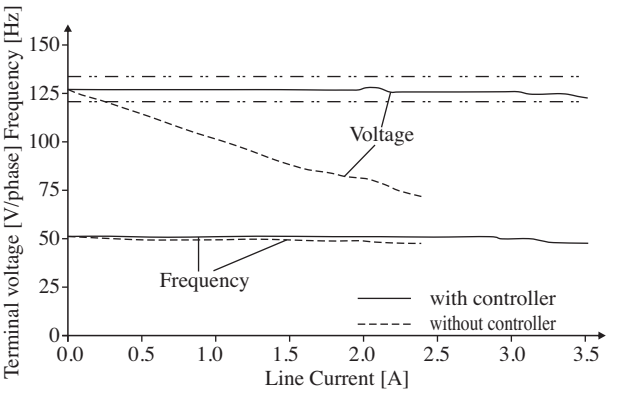

Figure 8. Steady-state performance of PVCEA under induction motor load.

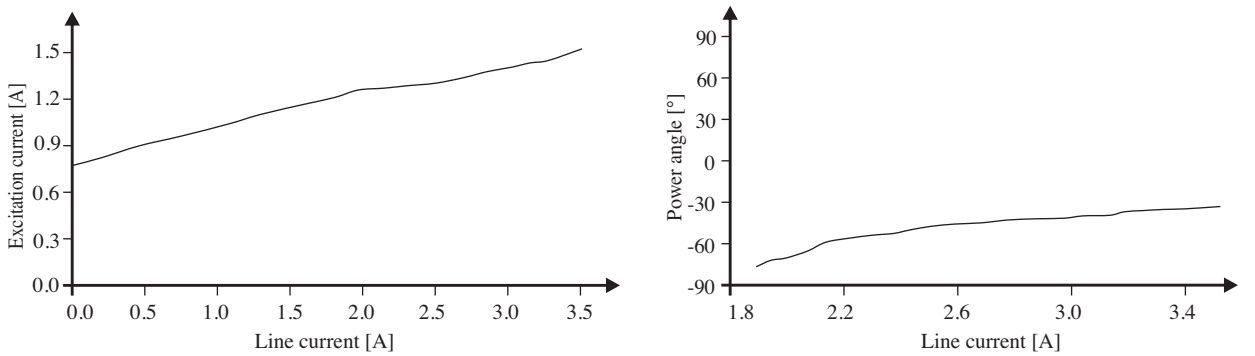

Figure 9. Excitation current and power angle characteristics of PVCEA under induction motor load (with controller).

As is well known, the current drawn by any electrical machine at the startup is higher than the nominal operating current. Due to the high current drawn at the startup, power consumption of the machine will be high, as well. The amount of this "high current" changes from one machine to another. In a study conducted in 2009 by Onat, Kıyak, and Gokmen, it was clearly concluded that the induction motor was the most compelling electrical machine for the power system. This motor demanded a startup power that was 2.14 times higher than the nominal power value. In addition, such a demand for high power (transient operation period) lasted for a long time of 6 s. On the other hand, the startup power of transformers was 1.3 times higher than the nominal value. Moreover, the time required to complete transient operation was only 1.5 s [16]. The effects of these characteristics are seen in sudden load experiment results. Especially in the startup, voltage falls to a very

large extent (up to 20% of nominal voltage) and the duration of stabilization is increased to 5 s. Despite the relatively low frequency reduction, duration of fluctuations is the same as voltage (with controller) (Figure 10).

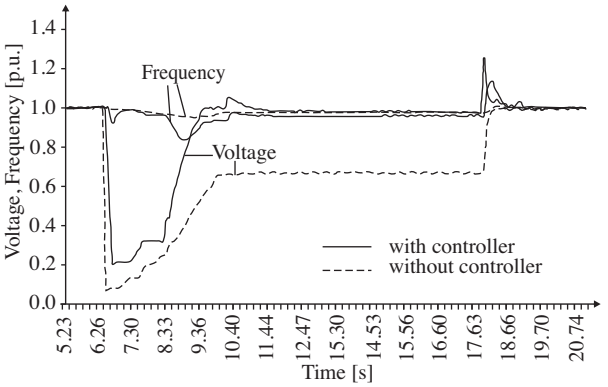

Figure 10. Transient voltage and frequency response of PVCEA under instantaneous induction motor load connection and disconnection.

Note that in steady-state operation, an asynchronous motor was gradually loaded with an eddy-current brake. We examined the behavior of the system in sudden loading situations by suddenly taking the asynchronous motor into the circuit with the shaft in the idle position.

3.4. Fault experiments

Synchronous generators, in the case of a sudden short circuit, may not be damaged for a few seconds after a fault because they possess high transient and subtransient reactance. Meanwhile, either the fault is eliminated or the generator is taken out of the circuit. We examined the response of the PVCEA to 3 different short-circuit faults. Short circuits were created while the motor was operating under its rated load.

As can be seen, the system was able to maintain frequency stability with a 1-phase ground short circuit, but the voltage decreased tremendously. To a large extent, similar observations can be made for the 3-phase short circuit. The machine seemed to be at inductive load in the case of short circuit. Therefore, while there was no change in frequency stability, large voltage reductions occurred.

4. Conclusions

Photovoltaic systems will be the preferential technologies in the long term as a result of developments made in semiconductive technology and use of nanomaterials. With the expansion of the use of PV systems, environmental problems can be reduced. In this study, we demonstrated that the PVCEA system, which was designed for use in small power plants, produces high quality electric power with constant voltage and frequency. In this design, a structure different from the classical hybrid systems was used. Excitation losses of a synchronous generator were obtained from PV modules. Thus, the electrical output of the generator was increased.

The design features 2 control systems with proportional integral (PI) controllers, making adjustments to voltage and frequency using pulse-width modulation (PWM). These control units keep the voltage and frequency stable under resistive load. The voltage and frequency controllers also successfully controlled the system under inductive load, the worst possible load situation faced by alternators for the purposes of voltage regulation.

This highlights the importance of voltage and frequency control circuits for the system, as an asynchronous motor load in a system without a controller can cause large voltage decreases.

The system, designed for the resistive and inductive load, was able to rapidly adapt to sudden load spikes, regaining voltage and frequency stability in a very short time. Stability was maintained throughout the period of operation. Although the system responded more slowly to the asynchronous motor load than to the other load scenarios, the desired performance was nevertheless obtained.

Our system design allows more flexible operating conditions due to the quality of the electric power it produces compared to small systems containing an asynchronous generator. In asynchronous generator stations containing a capacitor excitation system, the excitation current and voltage amplitude changes as capacity is adjusted. To control the capacity more finely, it is necessary to increase the capacitance number. This both increases the complexity of the system and causes excessive forcing of the control system. Our design is a good alternative for relatively low power applications containing an induction generator because of its sensitivity, quick reaction speed, and simple and reliable feedback circuits.

The system designed in this study brings a different approach to the hybrid operation of PV systems. Thus, a new field of application is revealed for stand-alone PV systems. In the design of PV systems, module and battery numbers are determined for the worst weather conditions of the study period. Therefore, excess energy that occurs in other operating times can meet intrasystem use or can be considered as a source of peak power. By increasing capacity utilization, the unit energy costs can be greatly reduced. Furthermore, the proposed system can also be applied to improve the energy efficiency of the systems in which the generators are used, such as mini- or microhydroelectric power plants, diesel systems, yachts, ferries, etc. Thus, a contribution to the reduction of fossil fuel consumption can be achieved.

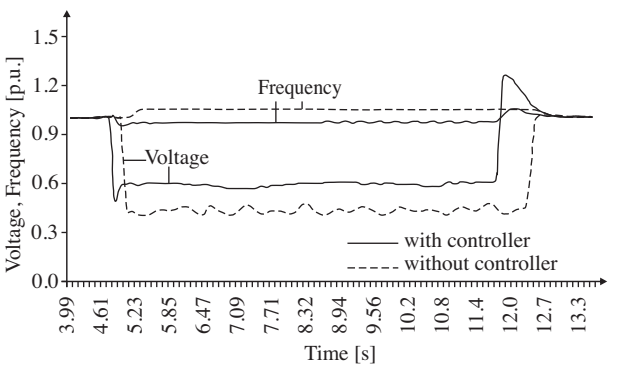

Figure 11. Transient voltage and frequency response of PVCEA under 1-phase-to-ground fault.

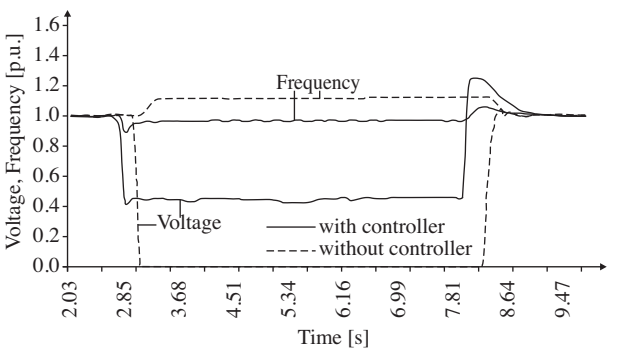

Figure 12. Transient voltage and frequency response of PVCEA to 3-phase short circuit.

Appendices

1. Calculations of PV system components

1.1. Determination of Load

To make the projection of any system, first the amount of energy demanded by the poles must be known. As the battery capacity is stated as *ampere-hour (Ah)*, the energy demand of the pole should be fixed as *Ah*. The common equation used to calculate the amount of daily demanded load is given in Eq. (1).

$$W = \left(\frac{kWh/year}{365} \cdot 1000 \right) \cdot \frac{1}{V_{ii}} \cdot \frac{1}{\eta_i} \cdot \frac{1}{\eta_w} \cdot \frac{1}{\eta_b} \tag{1}$$

1.2. Battery selection

The number of days requiring critical demand practice in photovoltaic systems depends on the area in which the system is set. Even at the least sunny times of the year, it can need less storage depending on the area. If the minimum hours of noon in the area during the operation hours of charge are known, the charge duration is calculated with the formulas below.

$$D_{critic} = -1.9T_{\min} + 18.3 \tag{2}$$

or,

$$D_{noncritic} = -0.48T_{\min} + 4.58 \tag{3}$$

Therefore, the battery capacity load could be written as:

$$B_{Ah} = W \cdot \frac{D}{D_T \cdot D_{ch} \cdot (disch)}. \tag{4}$$

Here, the D value is calculated with Eq. (2) or (3). For D_T in Eq. (4), it is pointed out that heat regulation factor D_{ch} points out the charge-discharge stated in the fraction. In this study, $D_T \cdot D_{ch} \cdot (disch) \approx 0.8$ is accepted. After finding the total battery capacity, the number of batteries that should be connected in a parallel manner is determined by dividing the total capacity into the battery capacity. It is not enough to just look at the cost in order to determine which battery is better. The designer should determine the service life of the battery.

In these formulae:

W : Daily demanded load [Ah/day]
V_{ii} : Inverter input voltage [V]
η_i : Inverter efficiency
η_w : Transmission efficiency
η_b : Battery efficiency
D : Number of storage days [days]
$T_{\min}$: Minimum peak sun hours [h/day]
B_{Ah} : Battery capacity [Ah]
D_{ch} : Charge-discharge correction factor
$disch$: Expressed as a fraction of discharge
D_T : Temperature correction factor

1.3. Panel sizing

PV panel can be sized often by determining the charge for each month of the year. This operation contains stages of assigning the proper slope for minimizing the system design stream and defining an acceptable amount of module, ensuring system current flow.

In order to obtain the system projection current, the regulated load is calculated for each month. It is necessary to consider the maximum and the minimum values of panel current in order to determine the optimum projection current. As it is essential for the system to be able to work under the worst conditions, the maximum current value should be chosen as the necessary projection current. This is the amount of the current that should be ensured by the photovoltaic panel.

The needed number of modules for the system is found by dividing the total projection current into the current of one module. After taking the probable loss caused by dust piling up over the years or by ageing into account, the projection current demanded from the panels is generally the value that is supplied by dividing the calculated current into an adjusted factor, decided as 0.9. The operation of rounding down this number is valid for batteries. In the selection of the modules, it is generally rounded up [17, 18].

1.4. Calculations

In this study, the system was located within the province of İstanbul and worked an average of 8 h/day in the most adverse climatic conditions during the experimental applications. Other variables are $V_{ii} = 24$ V, $\eta_i = \eta_b = 0.95$, and $\eta_w = 0.98$.

The worst time slot of average daily sunlight duration for İstanbul is January, at 2.25 h/day, according to statistical data from the State Meteorology Service [19]. In this case, by using Eqs. (1-4), the parameters are calculated as below.

Daily load demand, $W = 220 \cdot 1.4 \cdot 4 \cdot \frac{1}{24} \cdot \frac{1}{0.95} \cdot \frac{1}{0.95} \cdot \frac{1}{0.98} = 58Ah/day$.

Storage day number, $D_{noncritic} = -0.48 \cdot 2.25 + 4.58 = 3.5\ days$.

Total battery capacity, $B_{Ah} = 58 \cdot \frac{3.5}{0.8} = 253.75Ah$.

Necessary battery number, $253/100 = 2.53 \approx 2$.

Design current demanded from PV cells, $I = 58/\left(2.25 \cdot 0.9\right) = 28.6A$.

Number of modules, $28.6/6.85 = 4.18 \approx 4$.

Note that the excitation power of the alternator used in the experiments is quite high (308 VA). This value is bitwise equal to 25% nominal power, whereas the excitation power of large alternators produced commercially ($>$10 kVA) changes between 0.2 -1% of the nominal power [20, 21]. In this case, the required number of modules and batteries will be much lower.

2. Load values and connections

Grade values of resistive and inductive loads used in the experiments are given in Table 3. Connection diagrams are also seen in Figure 13. Photographs of the experimental setup are given in Figure 14.

Table 3. Grade values of resistive and inductive loads used in experiments.

Group		Measurement Frequency	Grades							Unit
			1	2	3	4	5	6	7	
Resistive Loads										
1	R-1	50 Hz	1090	779	464	324	237	176	149	Ω
	R-2		1065	758	443	309	220	153.5	128	
	R-3		1068	768	447	304.5	218	157	130	
2	R-1		1076	766	448	306	219	161	133	
	R-2		1071	768	447	304	218	154	128	
	R-3		1040	768	447	309	220.5	154.5	129	
Inductive Loads										
1	L-1	120 Hz	2939	2151	1261	872	661.4	482.6	395.4	mH
	L-2		2928	2144	1258	871	662.3	484.5	396.7	
	L-3		2956	2163	1269	877	665.2	485.5	397.9	
2	L-1		2825	2067	1208	871.7	637.7	466.6	381.9	
	L-2		2760	2015	1181	849.1	620.6	453	371.6	
	L-3		2867	2097	1230	879.7	642.8	449.7	384.6	

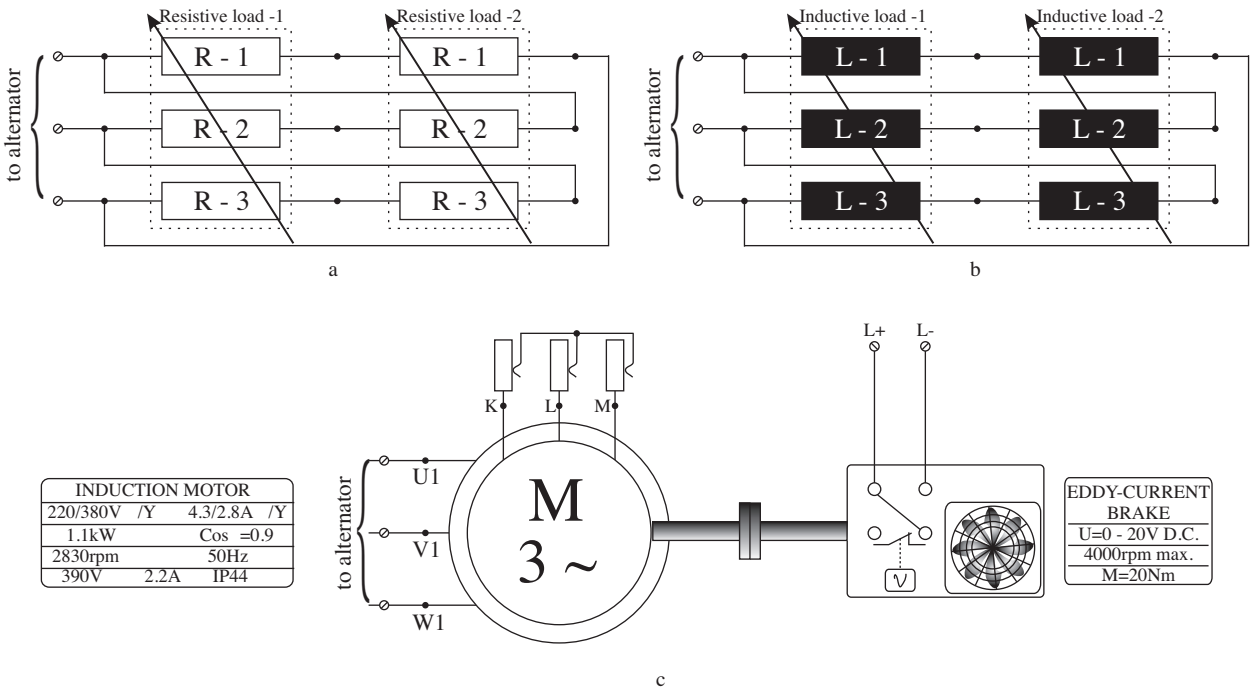

Figure 13. Load connections: a) resistive load, b) inductive load, c) induction motor and eddy-current brake.

Figure 14. Experimental setup: a) battery group, charge regulator, and fuses; b) solar panel; c) measurement tools and controllers; d) alternator, loads, and inverter.

References

[1] N.S. Sisworahardjo, M.Y. El-Sharkh, M.S. Alamb, "Neural Network Controller for Microturbine Power Plants", Electric Power Systems Research, Vol. 78, pp. 1378-1384, 2008.

[2] F. Shu, M. Chengxiong, C. Luonan, "Optimal Coordinated Pet and Generator Excitation Control for Power Systems", International Journal of Electrical Power and Energy Systems, Vol. 28, pp. 158-165, 2006.

[3] W.L. Brogan, Modern Control Theory, New Jersey, Prentice Hall, 1991.

[4] E. Campero-Littlewood, G. Espinosa-Perez, R. Escarela-Perez, "Transient Analysis of a Synchronous Generator Using a High-Order State Space Representation", Electronics, Robotics and Automotive Mechanics Conference, Vol. 2, pp. 258-263, 2006.

[5] P.P. Reichmeider, Investigations on the Internal Faults in Synchronous Machines, D.Eng., Rensselaer Polytechnic Institute, 2003.

[6] M.G. McArdle, D.J. Morrow, P.A.J. Calvert, O. Cadel, "A Fuzzy Tuning PID Automatic Voltage Regulator for Small Salient Pole Alternators", International Conference on Power System Technology Proceedings, Vol. 1, pp. 103-108, 2000.

[7] E.S. Mora, T.A. Olivares, D.R. Vega, D.A. Salinas, "The Effect of Induction Generators on the Transient Stability of a Laboratory Electric Power System", Electric Power Systems Research, Vol. 61, pp. 211-219, 2002.

[8] B.S. Borowy, Design and Performance Analysis of a Stand-Alone Wind/Photovoltaic Hybrid System, D.Eng., University of Massachusetts - Lowell, 1996.

[9] F. Giraud, Analysis of a Utility-Interactive Wind-Photovoltaic Hybrid System with Battery Storage Using Neural Network, D.Eng., University of Massachusetts - Lowell, 1999.

[10] V.N. Vasinanukom, Turbine-Governor and Exciter Control of DC Motor-Generator Set, M.S., University of Texas at Arlington, 2004.

[11] S.G.J. Ehnberg, "Reliability of a Small Power System Using Solar Power and Hydro", Electric Power System Research, Vol. 74, pp. 119-127, 2005.

[12] R. Muhida, A. Mostovan, W. Sujatmiko, M. Park, K. Matsuura, "The 10 Years Operation of a PV-Micro-Hydro Hybrid System in Taratak, Indonesia", Solar Energy Materials & Solar Cells, Vol. 67, pp. 621-627, 2001.

[13] H.H. Khalid, M. Itsuya, H. Tsutomu, O. Manabu, "Field and Armature Control for Separately Excited DC Motors by Photovoltaic Cells", IEEE Photovoltaic Energy Conversion Conference Record, Vol. 1, pp. 1169-1172, 1994.

[14] V. Vongmanee, V. Monyakul, U. Youngyuan, "Vector Control of Induction Motor Drive System Supplied by Photovoltaic Arrays", IEEE International Conference on Communications, Circuits and Systems, Vol. 2, pp. 1753-1756, 2002.

[15] R. Bonert, S. Rajakaruna, "Self-Excited Induction Generator with Excellent Voltage and Frequency Control", IEE Proceedings: Generation, Transmission, Distribution, Vol. 145, pp. 33-39, 1998.

[16] N. Onat, İ. Kıyak, G. Gökmen, "Experimental Wavelet Transient-State Analysis of Electrical Machines Directly Feeding by Photovoltaic Cells", WSEAS Transactions on Circuits and Systems, Vol. 8, pp. 719-728, 2009.

[17] R. Messenger, J. Ventre, Introduction to PV Systems, Chapter 7, Florida, CRC Press LLC, 2000.

[18] J.K. Kaldellis, K.A. Kavadias, P.S. Koronakis, "Comparing Wind and Photovoltaic Stand-Alone Power Systems Used for the Electrification of Remote Consumers", Renewable and Sustainable Energy Reviews, Vol. 11, pp. 57-77, 2007.

[19] Turkish Statistical Institute, Daily peak sun hour data: 30-year averages between 1975 and 2005, Ankara, 2005.

[20] T. Boduroğlu, Elektrik Makinaları Dersleri: Senkron Makinaların Hesap ve Konstrüksiyonu, Cilt. 3, İstanbul, 1994.

[21] Z. Jurin, B. Brkljac, M. Kolic, M. Kajari, V. Cesic, "Excitation Systems for High Power Synchronous Generators with Redundant Configurations", Proceedings of the 7. Konferenca Slovenskih Elektroenergetikov, pp. 55-60, Velenje, 2005.